

# Nanomolar Inhibitors of CNS Epinephrine Biosynthesis: (*R*)-(+)-3-Fluoromethyl-7-(*N*-substituted aminosulfonyl)-1,2,3,4-tetrahydroisoquinolines as Potent and Highly Selective Inhibitors of Phenylethanolamine *N*-Methyltransferase<sup>1</sup>

Gary L. Grunewald,\* F. Anthony Romero, and Kevin R. Criscione

Department of Medicinal Chemistry, University of Kansas, 1251 Wescoe Hall Drive, Lawrence, Kansas 66045

Received May 28, 2004

A series of (*R*)-(+)-3-fluoromethyl-7-(*N*-substituted aminosulfonyl)-1,2,3,4-tetrahydroisoquinolines has been synthesized and evaluated as inhibitors of PNMT and for their affinity for the  $\alpha_2$ -adrenoceptor. Compounds (*R*)-**8** and (*R*)-**9** are remarkably potent and selective inhibitors of PNMT and are predicted to penetrate the blood–brain barrier on the basis of their calculated log *P* values. Conformational analysis and docking studies were performed in order to examine why the (*R*)-enantiomer of these 3-fluoromethyl-7-(*N*-substituted aminosulfonyl)-1,2,3,4-tetrahydroisoquinolines is more potent than the (*S*)-enantiomer and to determine the likely bound ring conformer of the (*R*)-enantiomer. It appears that the (*R*)-enantiomer participates in a water-mediated hydrogen bond in which the (*S*)-enantiomer cannot. The likely favored ring conformation for (*R*)-3-fluoromethyl-7-(*N*-substituted aminosulfonyl)-1,2,3,4-tetrahydroisoquinolines in the PNMT active site is similar to the ring conformation of (*R*)-**5a** as determined by gas-phase ab initio calculations.

## Introduction

Epinephrine (Epi, **1**) was identified in the central nervous system (CNS) 50 years ago and was found to constitute approximately 5% of the total catecholamine content in the mammalian brain,<sup>2,3</sup> yet to this day, its role therein remains unclear. It has been implicated in some of the neurodegeneration seen in Alzheimer's disease,<sup>4,5</sup> as well as in the regulation of blood pressure,<sup>6</sup> respiration,<sup>7,8</sup> body temperature,<sup>7,8</sup> the  $\alpha_1$ -adrenoceptor,<sup>9</sup> and the  $\alpha_2$ -adrenoceptor.<sup>10,11</sup>

As part of our research program to elucidate the role of CNS Epi (**1**), we have targeted phenylethanolamine *N*-methyltransferase (PNMT: EC 2.1.1.28),<sup>2</sup> the terminal enzyme in the biosynthesis of Epi (**1**). This reaction involves the transfer of an activated methyl group from *S*-adenosyl-L-methionine (**2**) to the primary amine of norepinephrine (**3**) to produce Epi (**1**) and the cofactor product, *S*-adenosyl-L-homocysteine (AdoHcy, **4**). Some concerns with current PNMT inhibitors are (1) their selectivity for PNMT versus the  $\alpha_2$ -adrenoceptor and (2) their ability to penetrate into the CNS. A useful pharmacological tool to help define the role of CNS Epi (**1**) would be a potent inhibitor of PNMT that is selective and capable of crossing the blood–brain barrier (BBB).

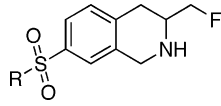
(±)-7-Aminosulfonyl-3-fluoromethyl-1,2,3,4-tetrahydroisoquinoline (**5**) is a highly potent and selective PNMT inhibitor (Table 1).<sup>12</sup> However, this compound may be too polar to penetrate into the CNS as indicated by BBB model studies and would not be useful as a pharmacological tool.<sup>12–14</sup> A calculated log *P*<sup>15</sup> (ClogP)

greater than 0.5 is likely required for 1,2,3,4-tetrahydroisoquinoline-type (THIQ) PNMT inhibitors in order to observe significant penetration into the CNS.<sup>12</sup> A previous study showed that adding nonpolar substituents to the sulfonamide nitrogen of **5** led to inhibitors (**6–11**) that were able to retain PNMT inhibitory potency and selectivity and, on the basis of their ClogP values, are predicted to cross the BBB (Table 1).<sup>16</sup> We proposed, on the basis of docking studies using the recently solved crystal structure (Figure 1) of human PNMT<sup>17</sup> (hPNMT) cocrystallized with SK&F 29661 (**13**; 7-aminosulfonyl-1,2,3,4-tetrahydroisoquinoline) and AdoHcy (**4**), that the 3-fluoromethyl moiety of 3-fluoromethyl-7-(*N*-substituted aminosulfonyl)-1,2,3,4-tetrahydroisoquinolines is making a hydrophobic contact with Tyr222 and the substituent on the sulfonamide nitrogen is binding in an auxiliary binding pocket. The auxiliary binding pocket appears to favor lipophilic alkyl chains that contain a trifluoromethyl moiety at the terminus, as exemplified by **8** (Figure 2). In that study, **8** and **9** were the most potent and selective PNMT inhibitors reported.

We have previously reported the synthesis and evaluation of the enantiomers of **12**,<sup>18</sup> and it was observed that (*R*)-**12** was more potent than (*S*)-**12** at PNMT. Interestingly, it was also noted that (*R*)-**12** and (*S*)-**12** (Table 1) were equipotent at the  $\alpha_2$ -adrenoceptor. Therefore, we wanted to investigate other (*R*)-*N*-substituted analogues of **5**. If this same trend in equipotency at the  $\alpha_2$ -adrenoceptor is observed, then it would be possible to produce enantiopure 3-fluoromethyl-7-(*N*-substituted aminosulfonyl)-THIQs that have nanomolar PNMT inhibitory potency and increased selectivity.

**Chemistry.** Sulfonyl chloride **14**<sup>18</sup> was a common starting material which could be readily converted to the desired enantiopure sulfonamides. The synthesis of

\* To whom correspondence should be addressed: Gary L. Grunewald, Department of Medicinal Chemistry, School of Pharmacy, Malott Hall, Room 4060, University of Kansas, 1251 Wescoe Hall Dr., Lawrence, KS 66045-7582. Phone: (785) 864-4497. Fax: (785) 864-5326. E-mail: ggrunewald@ku.edu.

**Table 1.** In Vitro Activities of 3-Fluoromethyl-7-*N*-(substituted aminosulfonyl)-THIQs


compd	R	PNMT: $K_i$ ( $\mu\text{M}$ ) $\pm$ SEM	$\alpha_2^a$ : $K_i$ ( $\mu\text{M}$ ) $\pm$ SEM	selectivity: $\alpha_2/\text{PNMT}$	ClogP <sup>b</sup>
( $\pm$ )- <b>5</b> <sup>c,d</sup>	NH <sub>2</sub>	0.15 $\pm$ 0.01	680 $\pm$ 10	4,500	0.00
( $\pm$ )- <b>6</b> <sup>e</sup>	NHCH <sub>2</sub> CH <sub>3</sub>	1.4 $\pm$ 0.1	550 $\pm$ 60	390	1.15
( $\pm$ )- <b>7</b> <sup>e</sup>	NHCH <sub>2</sub> CH <sub>2</sub> CH <sub>3</sub>	1.7 $\pm$ 0.2	610 $\pm$ 60	360	1.67
( $\pm$ )- <b>8</b> <sup>e</sup>	NHCH <sub>2</sub> CF <sub>3</sub>	0.13 $\pm$ 0.02	1200 $\pm$ 100	9200	1.41
( $\pm$ )- <b>9</b> <sup>e</sup>	NHCH <sub>2</sub> CH <sub>2</sub> CF <sub>3</sub>	0.22 $\pm$ 0.02	660 $\pm$ 80	3000	1.39
( $\pm$ )- <b>10</b> <sup>e</sup>	NH(CH <sub>2</sub> ) <sub>3</sub> OCH <sub>3</sub>	2.6 $\pm$ 0.2	750 $\pm$ 70	290	0.98
( $\pm$ )- <b>11</b> <sup>e</sup>	N(CH <sub>2</sub> CH <sub>2</sub> ) <sub>2</sub> S	1.2 $\pm$ 0.2	190 $\pm$ 20	160	1.71
( $\pm$ )- <b>12</b> <sup>d,e</sup>	NH(4-Cl-Ph)	0.27 $\pm$ 0.02	140 $\pm$ 20	520	3.18
( <i>R</i> )-(+)- <b>12</b> <sup>d,f</sup>	NH(4-Cl-Ph)	0.11 $\pm$ 0.01	140 $\pm$ 20	1270	3.18
( <i>S</i> )-(+)- <b>12</b> <sup>d,f</sup>	NH(4-Cl-Ph)	0.61 $\pm$ 0.08	150 $\pm$ 20	250	3.18

<sup>a</sup> In vitro activities reported for the inhibition of binding of [<sup>3</sup>H]clonidine at the  $\alpha_2$ -adrenoceptor. <sup>b</sup> Calculated log *P*. <sup>c</sup> Reference 12. <sup>d</sup> The biochemical data was reported earlier for bovine PNMT. It is reported here for recombinant human PNMT. <sup>e</sup> Reference 16. <sup>f</sup> Reference 18.

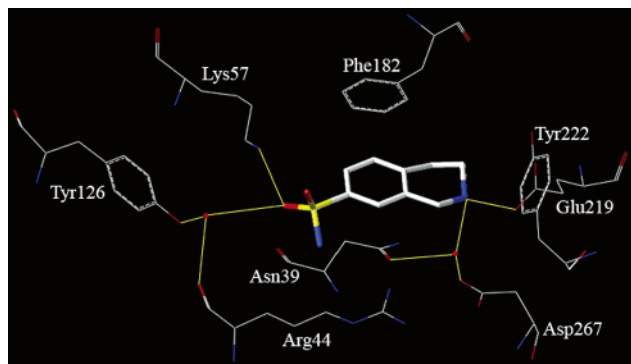
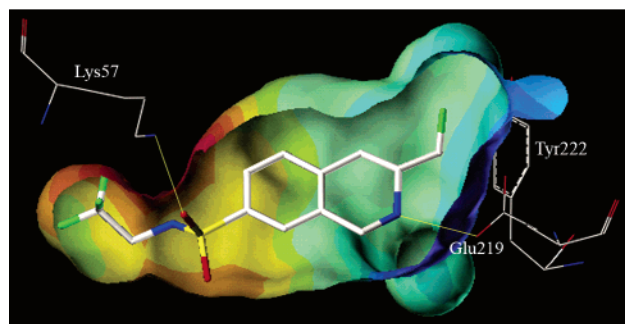
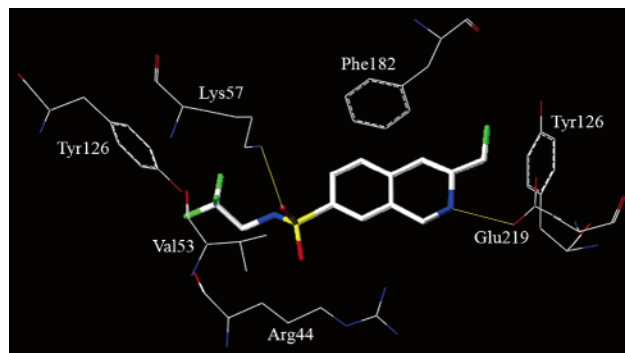


**Figure 1.** This figure shows the amino acid residues and water molecules that could interact with SK&F 29661 (**13**) within the hPNMT active site. Yellow lines indicate possible hydrogen bonds. Carbon is white, nitrogen is blue, oxygen is red, and sulfur is yellow. Water molecules are indicated by a red dot. Hydrogens are not shown for clarity.

**14** employed the use of (*R*)-(+)-phenylalanine to establish the chiral center. Sulfonyl chloride **14** was treated with ammonium hydroxide in acetonitrile to yield **15** (Scheme 1). Sulfonamides **16**–**21** were produced by treatment of **14** with the requisite amine in a biphasic mixture of EtOAc and saturated sodium carbonate. In the case of **8** and **9**, yields were improved with the addition of 4 equiv of pyridine to the reaction. No further purification of the resultant sulfonamide was required. Reduction of **15**–**21** with BH<sub>3</sub>·THF yielded the corresponding THIQs (*R*)-**5**–(*R*)-**11**.<sup>19</sup>

**Biochemistry.** In the current study, human PNMT (hPNMT) was expressed in *E. coli*<sup>20</sup> and purified with a C-terminal hexahistidine tag.<sup>16</sup> The radiochemical assay conditions, previously reported for the bovine enzyme,<sup>21</sup> were modified to account for the high binding affinity of some inhibitors. Inhibition constants were determined using four concentrations of phenylethanolamine as the variable substrate, and three concentrations of inhibitor.

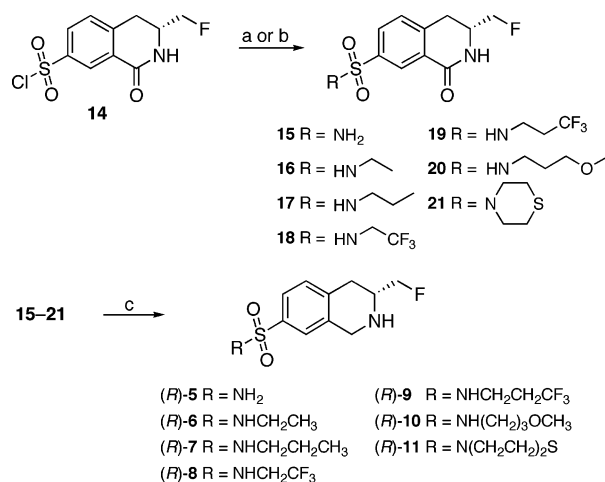
$\alpha_2$ -Adrenergic receptor binding assays were performed using cortex obtained from male Sprague Dawley rats.<sup>22</sup> [<sup>3</sup>H]Clonidine was used as the radioligand to define the specific binding and phentolamine was used to define the nonspecific binding. Clonidine was used as the ligand to define  $\alpha$ -adrenergic binding affinity to simplify the comparison with previous results.



**Figure 2.** Part A (top) shows (*R*)-**8** docked into the hPNMT active site. Part B (bottom) is an electrostatic potential mapped on the Connolly (solvent accessible) surface of the hPNMT active site revealing (*R*)-**8**. The red-orange area indicates where electron density is favored, whereas the blue area indicates where electron density is disfavored. Green indicates neutrality. Carbon is white, nitrogen is blue, fluorine is green, oxygen is red, and sulfur is yellow. Hydrogens are not shown for clarity.

## Results and Discussion

Compounds (*R*)-**5**–(*R*)-**11** were evaluated for their inhibitory potency at PNMT and for their affinity for the  $\alpha_2$ -adrenoceptor (Table 2). As expected, these enantiopure sulfonamides displayed excellent PNMT inhibitory potency, being approximately twice as potent at PNMT as their corresponding racemate. In general, for 3-fluoromethyl-7-*N*-(substituted aminosulfonyl)-THIQs, there is no stereoselective bias for the  $\alpha_2$ -adrenoceptor with the (*R*)-enantiomer being just as potent as the racemate. Since PNMT inhibitory potency increases while the  $\alpha_2$ -adrenoceptor affinity stays the same for these (*R*)-3-fluoromethyl-7-*N*-(substituted aminosulfonyl)-THIQs, twice the selectivity is observed as com-

Scheme 1<sup>a</sup>

<sup>a</sup> Primary or secondary amines, EtOAc/Na<sub>2</sub>CO<sub>3</sub>; (b) NH<sub>4</sub>OH, MeCN; (c) BH<sub>3</sub>·THF.

pared to the racemate. Compound (*R*)-**8** has a selectivity (16 000) that far surpasses any compound previously reported.

We wished to examine in 3-fluoromethyl-7-(*N*-substituted aminosulfonyl)-THIQs why the (*R*)-enantiomer is more potent than the (*S*)-enantiomer at PNMT and to determine the likely bound ring conformer of the (*R*)-enantiomer in the PNMT active site. A previous study on substituted 3-phenyl-1,2,3,4-tetrahydroisoquinolines found that the half chair conformer was lower in energy than the boat conformer (at least a 2.50 kcal/mol difference).<sup>23</sup> Assuming this holds true for *rac*-**5**, there are four possible ring conformations for each configuration of **5** (Figure 3). These four conformations arise from the two-half chair conformers and the combination of axial/equatorial orientations of the 3-fluoromethyl group and the THIQ nitrogen lone pair. Figure 3A shows the (*R*)-configuration of the four conformations and Figure 3B shows the (*S*)-configuration of the four conformations. Snyder et al. have previously examined the NH–FC dipole orientation of **6** and found that the low energy C–C(F) rotamer (similar to (*R*)-**5a** in Figure 3A) aligns the fluorine with the equatorial hydrogen on the THIQ nitrogen allowing for electrostatic stabilization.<sup>24</sup> This study was performed on **6** in its protonated form, but, as previous studies suggest that the THIQ amine does not bind protonated to PNMT,<sup>25,26</sup> we performed the conformational analysis of **5** on its neutral form. The relative energy was determined for each conformer of **5** using Gaussian 98<sup>27</sup> with the

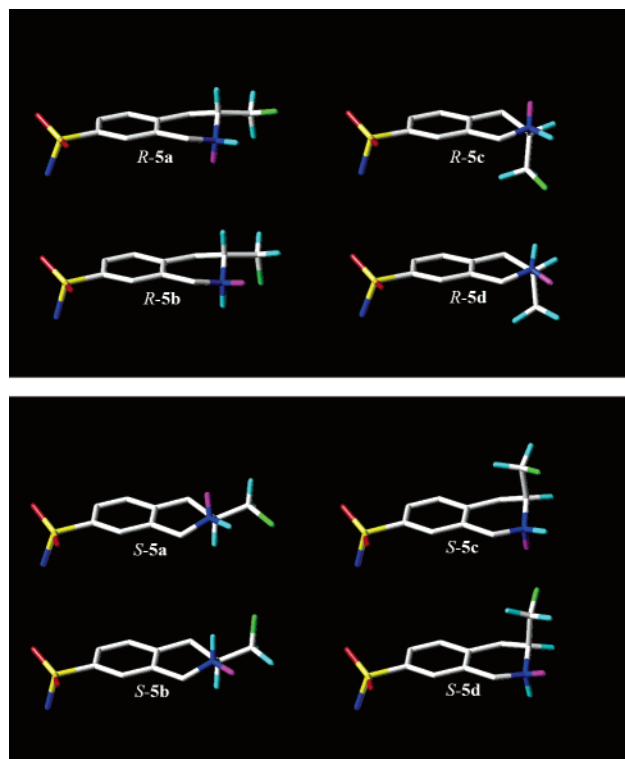


**Figure 3.** Geometry optimized (see Experimental Section) conformations of (*R*)-**5** (top) and (*S*)-**5** (bottom). Carbon is white, nitrogen is blue, hydrogen is cyan, the lone pair is magenta, fluorine is green, sulfur is yellow, and oxygen is red. Some hydrogens are not shown for clarity.

6-31G\* basis set (see experimental) and is shown in Table 3. The lowest energy C–C(F) rotamer for each conformer was one in which the fluorine aligns with the hydrogen on the THIQ nitrogen, except for (*R*)-**5d**/*S*)-**5d** which cannot assume such an alignment. The global minimum was determined to be (*R*)-**5a**/*S*)-**5a** in which the 3-fluoromethyl group is equatorial and THIQ nitrogen lone pair is axial. This is the same low energy conformer and rotamer determined in the earlier study<sup>24</sup> of **6** in the protonated form and is also consistent with a study on the conformational analysis of substituted 3-phenyl-1,2,3,4-tetrahydroisoquinolines.<sup>23</sup> Compound (*R*)-**5a**/*S*)-**5a** is a likely candidate that would be favored in the PNMT active site.

To examine why (*R*)-**5** is favored in the PNMT active site and to determine the favored conformation of (*R*)-**5**, all four conformations for each configuration of **5** were docked<sup>28</sup> (see Experimental Section) into the crystal structure of hPNMT<sup>17</sup> cocrystallized with SK&F 29661

**Table 2.** In Vitro Activities of (*R*)-(+)-3-Fluoromethyl-7-*N*-(substituted aminosulfonyl)-THIQs

compd	R	PNMT: $K_1$ ( $\mu$ M) $\pm$ SEM	$\alpha_2^a$ : $K_1$ ( $\mu$ M) $\pm$ SEM	selectivity: $\alpha_2$ /PNMT	ClogP <sup>b</sup>
( <i>R</i> )- <b>5</b>	NH <sub>2</sub>	0.072 $\pm$ 0.006	700 $\pm$ 70	9700	0.00
( <i>R</i> )- <b>6</b>	NHCH <sub>2</sub> CH <sub>3</sub>	0.75 $\pm$ 0.06	550 $\pm$ 50	730	1.15
( <i>R</i> )- <b>7</b>	NHCH <sub>2</sub> CH <sub>2</sub> CH <sub>3</sub>	0.79 $\pm$ 0.11	570 $\pm$ 60	720	1.67
( <i>R</i> )- <b>8</b>	NHCH <sub>2</sub> CF <sub>3</sub>	0.061 $\pm$ 0.003	1000 $\pm$ 100	16000	1.41
( <i>R</i> )- <b>9</b>	NHCH <sub>2</sub> CH <sub>2</sub> CF <sub>3</sub>	0.099 $\pm$ 0.011	670 $\pm$ 80	6800	1.39
( <i>R</i> )- <b>10</b>	NH(CH <sub>2</sub> ) <sub>2</sub> OCH <sub>3</sub>	1.2 $\pm$ 0.1	680 $\pm$ 80	570	0.98
( <i>R</i> )- <b>11</b>	N(CH <sub>2</sub> ) <sub>2</sub> S	0.61 $\pm$ 0.06	200 $\pm$ 20	330	1.71

<sup>a</sup> In vitro activities reported for the inhibition of binding of [<sup>3</sup>H]clonidine at the  $\alpha_2$ -adrenoceptor. <sup>b</sup> Calculated log *P*.

**Table 3.** Energies<sup>a</sup> for 7-Aminosulfonyl-3-fluoromethyl-THIQ (5)

compd	orientation of THIQ nitrogen lone pair	orientation of fluoromethyl	$\Delta$ energy <sup>b</sup> (kcal/mol)
( <i>R</i> )-5a	axial	equatorial	0.0
( <i>R</i> )-5b	equatorial	equatorial	2.9
( <i>R</i> )-5c	axial	axial	3.2
( <i>R</i> )-5d	equatorial	axial	2.6

<sup>a</sup> Gaussian 98/6-31G\*. <sup>b</sup> Difference in energy from global minimum (*R*)-5a.

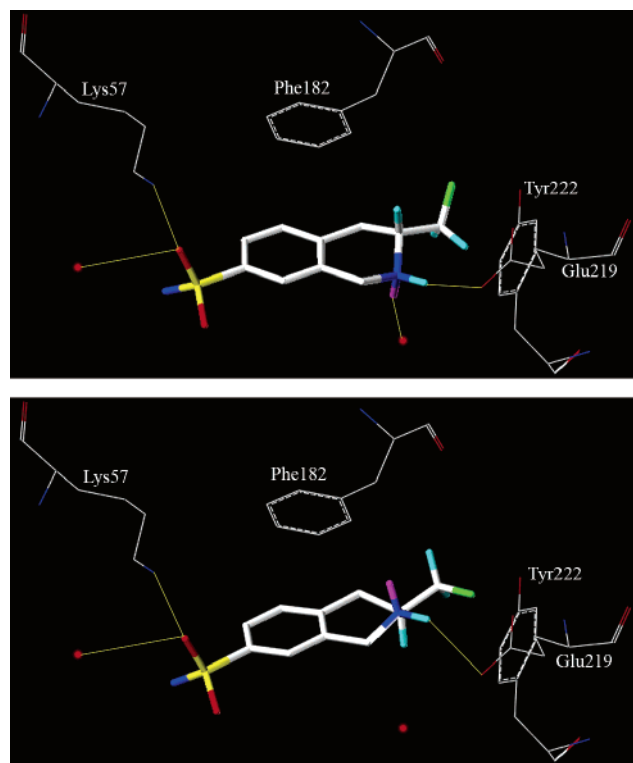


**Figure 4.** Part A (top) shows (*R*)-5a docked into the hPNMT active site. Part B (bottom) shows (*S*)-5a docked into the hPNMT active site. Yellow lines indicate possible hydrogen bonds. Carbon is white, nitrogen is blue, hydrogen is cyan, oxygen is red, fluorine is green, lone pair is magenta, and sulfur is yellow. Water is indicated by a red dot. Some hydrogens are not shown for clarity.

(13) and AdoHcy (4; selected structures shown in Figures 4 and 5). If we assume that PNMT ligands bind neutral in the PNMT active site, then only when the hydrogen on the THIQ nitrogen is equatorial (lone pair axial) can it hydrogen bond with Glu219 (Figures 4 and 5). This is consistent with a previous study on a set of conformationally defined benzylamines in which there is a correlation between the direction of the lone pair and PNMT  $K_i$ . In that study, it was found that PNMT inhibitory potency dramatically increased with benzylamine analogues that possess an axial lone pair.<sup>29</sup> On the sole basis of the fact that the lone pair on the THIQ nitrogen must be axial in order for the ligand to be a potent PNMT inhibitor, only (*R*)-5a, (*S*)-5a, (*R*)-5c and (*S*)-5c meet this requirement. Compounds (*R*)-5a/*S*-5a and (*R*)-5c/*S*-5c are different in respect to the space in the active site where the 3-fluoromethyl moiety resides. Docking studies indicate that the fluoromethyl moiety of (*R*)-5a/*S*-5a can make a hydrophobic contact with Tyr222 (Figure 4). Conversely, in (*R*)-5c/*S*-5c, the fluoromethyl moiety cannot make this hydrophobic

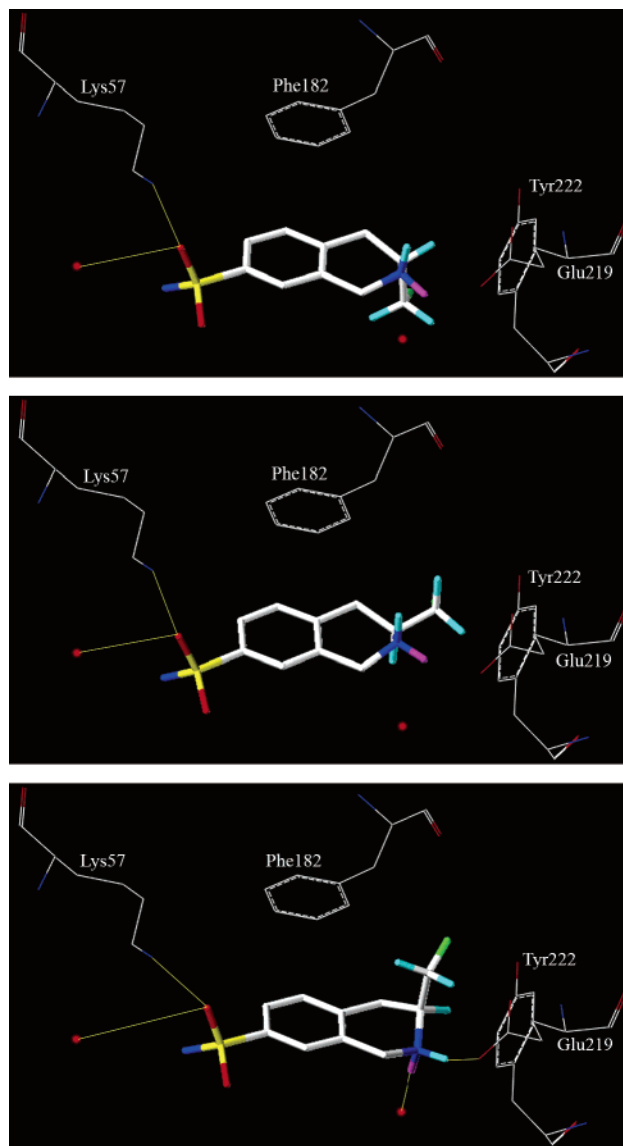


**Figure 5.** Part A (top) shows (*R*)-5d docked into the hPNMT active site. Part B (middle) shows (*S*)-5b docked into the hPNMT active site. Part C (bottom) shows (*S*)-5c docked into the hPNMT active site. Yellow lines indicate possible hydrogen bonds. Carbon is white, nitrogen is blue, hydrogen is cyan, oxygen is red, fluorine is green, lone pair is magenta, and sulfur is yellow. Water is indicated by a red dot. Some hydrogens are not shown for clarity.

contact, nor is it in the vicinity of other residues to make any other favorable contact (Figure 5). In addition, the conformation of (*R*)-5c/*S*-5c is not favored energetically (3.2 kcal above the global minimum; Table 3), which suggests it is not a likely conformer that would be favored in the PNMT active site. Only (*R*)-5a and (*S*)-5a appear to place the 3-fluoromethyl group and the hydrogen on the THIQ nitrogen in the optimal orientations to interact with the PNMT active site (Figure 4). Figure 6 is an overlay of (*R*)-5a and (*S*)-5a and shows how the appropriate groups that interact with the enzyme occupy a similar area of space. However, a visible difference in these structures is the location of the lone pair on the THIQ nitrogen. In the crystal structure of hPNMT,<sup>17</sup> the THIQ nitrogen of SK&F 29661 (13) makes a water-mediated hydrogen bond with Asn39 and Asp267. Compound (*R*)-5a can simultaneously participate in this water-mediated hydrogen

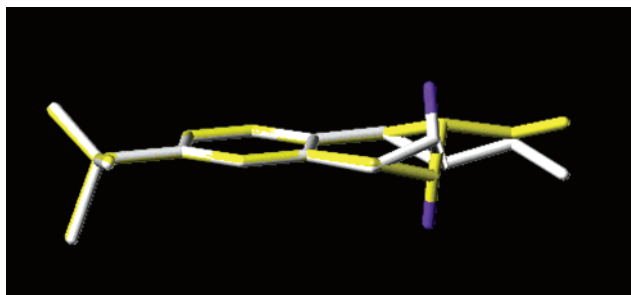


**Figure 6.** Overlay of (*R*)-**5a** (yellow) and (*S*)-**5a** (white). The atoms used for the fit were the aromatic carbon atoms. Nitrogen lone pair is purple. Hydrogens are not shown for clarity.

bond while maintaining optimal fluorine atom-PNMT contact, whereas (*S*)-**5a** cannot. This combination of interactions may explain the increased PNMT inhibitory potency for the (*R*)-enantiomer over the (*S*)-enantiomer. On the basis of the discussion presented above, we believe that the favored binding conformation of these (*R*)-3-fluoromethyl-7-(*N*-substituted aminosulfonyl)-THIQs in the PNMT active site is represented by the ring conformation of (*R*)-**5a**. Verification of this hypothesis will require a crystal structure of hPNMT cocrystallized with a (*R*)-3-fluoromethyl-7-(*N*-substituted aminosulfonyl)-THIQ.

In summary, we have prepared and evaluated a small set of (*R*)-3-fluoromethyl-7-(*N*-substituted aminosulfonyl)-THIQs for their potency and selectivity for PNMT versus the  $\alpha_2$ -adrenoceptor. Since PNMT inhibitory potency increases by approximately 2-fold for (*R*)-**5**–(*R*)-**11** and  $\alpha_2$ -adrenoceptor affinity stays the same for each enantiomer as compared to the racemate, twice the selectivity is observed between the enantiomer and racemate. Geometry optimization and docking studies indicate that the favored ring conformation of (*R*)-(+)-3-fluoromethyl-7-(*N*-substituted aminosulfonyl)-THIQs in the PNMT active site is similar to that determined by ab initio calculations for (*R*)-**5a**. Compounds (*R*)-**8** and (*R*)-**9** are two of the most potent and selective PNMT inhibitors reported to date and are predicted, on the basis of their ClogP values, to penetrate into the CNS. These compounds may prove useful as pharmacological tools to help elucidate the role of CNS Epi.

## Experimental Section

All of the reagents and solvents used were reagent grade or were purified by standard methods before use. Melting points were determined in open capillary tubes on a Thomas-Hoover melting point apparatus calibrated with known compounds but are otherwise uncorrected. All proton ( $^1\text{H}$  NMR) and carbon ( $^{13}\text{C}$  NMR) nuclear magnetic resonance spectra were taken on a Bruker DRX-400 or a Bruker AM-500 spectrometer. High-resolution mass spectra (HRMS) were obtained on a VG Analytical ZAB. All elemental analysis was performed by Quantitative Technologies, Inc. (Whitehouse, NJ). Flash chromatography was performed using silica gel 60 (230–400 mesh) supplied by Universal Adsorbents, Atlanta, GA. All methanol (MeOH) and ethanol (EtOH) used were anhydrous unless stated otherwise and were prepared by distillation over magnesium. Anhydrous tetrahydrofuran (THF) and diethyl ether ( $\text{Et}_2\text{O}$ ) were distilled from sodium–benzophenone ketyl. Hexanes refers to the mixture of hexane isomers (bp 40–70 °C). All reactions that required anhydrous conditions were performed under argon, and all glassware was either oven-dried or flame-dried before use. AdoMet was

obtained from Sigma-Aldrich (St. Louis, MO). [*methyl*- $^3\text{H}$ ]-AdoMet and [ $^3\text{H}$ ]clonidine were obtained from PerkinElmer (Boston, MA).

**Radiochemical Assay of PNMT Inhibitors.** The assay used in this study has been modified from that described previously.<sup>21</sup> A typical assay mixture consisted of 25  $\mu\text{L}$  of 0.5 M phosphate buffer (pH 8.0), 25  $\mu\text{L}$  of 50  $\mu\text{M}$  unlabeled AdoMet, 5  $\mu\text{L}$  of [*methyl*- $^3\text{H}$ ]AdoMet, containing approximately  $3 \times 10^5$  dpm (specific activity approximately 15 Ci/mmol), 25  $\mu\text{L}$  of substrate solution (phenylethanolamine), 25  $\mu\text{L}$  of inhibitor solution, 25  $\mu\text{L}$  of enzyme preparation (containing 30 ng of hPNMT and 25  $\mu\text{g}$  of bovine serum albumin), and sufficient water to achieve a final volume of 250  $\mu\text{L}$ . After incubation for 30 min at 37 °C, the reaction mixture was quenched by addition of 250  $\mu\text{L}$  of 0.5 M borate buffer (pH 10.0) and was extracted with 2 mL of toluene/isoamyl alcohol (7:3). A 1 mL portion of the organic layer was removed, transferred to a scintillation vial, and diluted with cocktail for counting. The mode of inhibition was ascertained to be competitive in all cases reported in Tables 1 and 2 by examination of the correlation coefficients ( $r^2$ ) for the fit routines as calculated in the Enzyme Kinetics module (version 1.1) in SigmaPlot (version 7.0).<sup>30</sup> While all  $K_i$  values reported were calculated using competitive kinetics, it should be noted that there was not always a great difference between the  $r^2$  values for the competitive model versus the noncompetitive model. All assays were run in duplicate with three inhibitor concentrations over a 5-fold range.  $K_i$  values were determined by a hyperbolic fit of the data using the Single Substrate–Single Inhibitor routine in the Enzyme Kinetics module (version 1.1) in SigmaPlot (version 7.0). For inhibitors with apparent  $\text{IC}_{50}$  values less than 0.1  $\mu\text{M}$  (as determined by a preliminary screen of the compounds to be assayed), the Tight Binding Inhibition routine was used to calculate the  $K_i$  values.

**$\alpha_2$ -Adrenoceptor Radioligand Binding Assay.** The radioligand receptor binding assay was performed according to the method of U'Prichard et al.<sup>22</sup> Male Sprague–Dawley rats were decapitated, and the cortexes were dissected out and homogenized in 20 volumes (w/v) of ice-cold 50 mM Tris/HCl buffer (pH 7.7 at 25 °C). Homogenates were centrifuged thrice for 10 min at  $50\,000 \times g$  with resuspension of the pellet in fresh buffer between spins. The final pellet was homogenized in 200 volumes (w/v) of ice-cold 50 mM Tris/HCl buffer (pH 7.7 at 25 °C). Incubation tubes containing [ $^3\text{H}$ ]clonidine (specific activity approximately 20 mCi/mmol, final concentration 2.0 nM), various concentrations of drugs, and an aliquot of freshly resuspended tissue (800  $\mu\text{L}$ ) in a final volume of 1 mL were used. Tubes were incubated at 25 °C for 30 min, and the incubation was terminated by rapid filtration under vacuum through GF/B glass fiber filters. The filters were rinsed with three 5 mL washes of ice-cold 50 mM Tris buffer (pH 7.7 at 25 °C). The filters were counted in vials containing premixed scintillation cocktail. Nonspecific binding was defined as the concentration of bound ligand in the presence of 2  $\mu\text{M}$  of phentolamine. All assays were run in quadruplicate with 5 inhibitor concentrations over a 16-fold range.  $\text{IC}_{50}$  values were determined by a log-probit analysis of the data and  $K_i$  values were determined by the equation  $K_i = \text{IC}_{50}/(1 + [\text{clonidine}]/K_D)$ , as all Hill coefficients were approximately equal to 1.

**Molecular Modeling.** Calculated log *P* (ClogP) values and Connolly surfaces were generated in SYBYL on a Silicon Graphics Octane workstation. Docking of the various inhibitors into the PNMT active site was performed using AutoDock 3.0.<sup>31</sup> The default settings for AutoDock were used. The initial structure for docking into the PNMT active site was the geometry optimized structure generated by Gaussian 98.<sup>27</sup> Geometry optimization and energy calculations for (*R*)-**5** were performed using Gaussian 98 with the 6-31G\* basis set. The starting geometry was a half chair conformation of (*R*)-**5** and was minimized with the Tripos force field before performing the geometry optimization. The energies for different rotamers were calculated using Gaussian 98/6-31G\* single point optimization.

**(R)-3-Fluoromethyl-7-aminosulfonyl-1,2,3,4-tetrahydroisoquinoline Hydrochloride (R-5·HCl).** Compound **14** (150 mg, 0.540 mmol) was dissolved in acetonitrile (10 mL) and  $\text{NH}_4\text{OH}$  (6.5 mL) was added and the reaction stirred overnight. The solvent was evaporated, and the residue was dissolved in saturated sodium bicarbonate and extracted with EtOAc. The organic layers were combined, washed twice with brine, and dried over  $\text{Na}_2\text{SO}_4$ . The solvent was evaporated to give crude lactam **15** (113 mg). Lactam **15** (113 mg, 0.438 mmol) was reduced with  $\text{BH}_3\cdot\text{THF}$  (1.75 mL, 1.75 mmol) in a similar procedure as described in the general procedure (vide infra) except the free amine was extracted at pH 10. Recrystallization of the HCl salt in EtOH/hexanes yielded (*R*)-**5**·HCl (50 mg, 33%). All spectral data were identical to those reported for the racemic compound:<sup>12</sup> mp 210–211 °C;  $[\alpha]_{\text{D}}^{22} = +118.7$  (*c* 0.15, MeOH); Anal. ( $\text{C}_{10}\text{H}_{13}\text{N}_2\text{O}_2\text{FS}\cdot\text{HCl}$ ) C, H, N.

**General Procedure for (R)-6–(R)-11 (selected procedure for (R)-7).** Sulfonyl chloride **14** (400 mg, 1.44 mmol) was dissolved in EtOAc (12 mL) and saturated  $\text{Na}_2\text{CO}_3$  (8 mL). In the case of compounds (*R*)-**8** and (*R*)-**9**, pyridine (4 equiv) was added to the reaction. *n*-Propylamine (355  $\mu\text{L}$ , 4.32 mmol) was added to the reaction mixture and stirred for 6 h. The organic phase was separated, and the aqueous phase was washed twice with EtOAc. The organic layers were combined, washed twice with 3 N HCl and brine, and dried over  $\text{Na}_2\text{SO}_4$ . The solvent was evaporated to give crude lactam **17** (368 mg, 89%). Lactam **17** was dissolved in THF (20 mL), and  $\text{BH}_3\cdot\text{THF}$  (5.12 mL, 5.12 mmol) was added. The solution was refluxed for 8 h and cooled with an ice–water bath. The reaction was quenched with the slow addition of MeOH (10 mL) and allowed to stir for 0.5 h. The solution was evaporated, and the oily residue was dissolved in MeOH (25 mL) and 6 N HCl (5 mL) and refluxed for 3 h. The MeOH was evaporated, and the aqueous layer was made basic with 15% NaOH. The aqueous layer was saturated with NaCl and extracted three times with EtOAc. The combined organic layers were washed with brine and dried over  $\text{Na}_2\text{SO}_4$ . The solvent was evaporated to give a crude residue which was dissolved in MeOH, and  $\text{HCl}_{(\text{g})}$  was bubbled through the solution. The MeOH was evaporated, and the solid was recrystallized from EtOH/hexanes to yield (*R*)-**7**·HCl as white crystals (250 mg, 64% from **14**). In some cases the free amine was purified by flash chromatography (DCM/MeCN as eluent) before conversion to the HCl salt.

**(R)-3-Fluoromethyl-7-(N-ethylaminosulfonyl)-1,2,3,4-tetrahydroisoquinoline Hydrochloride (R-6·HCl).** Sulfonyl chloride **14** (400 mg, 1.44 mmol) was reacted with ethylamine hydrochloride (354 mg, 4.34 mmol) to afford **16** (343 mg). Lactam **16** (343 mg, 1.26 mmol) was reduced with  $\text{BH}_3\cdot\text{THF}$  (5.0 mL, 5.0 mmol) to yield (*R*)-**6**·HCl (220 mg, 52%). All spectral data were identical to those reported for the racemic compound:<sup>16</sup> mp 248–249 °C;  $[\alpha]_{\text{D}}^{26} = +57.2$  (*c* 0.21, MeOH); Anal. ( $\text{C}_{12}\text{H}_{17}\text{N}_2\text{O}_2\text{FS}\cdot 0.25 \text{H}_2\text{O}\cdot\text{HCl}$ ) C, H, N.

**(R)-3-Fluoromethyl-7-(N-propylaminosulfonyl)-1,2,3,4-tetrahydroisoquinoline Hydrochloride (R-7·HCl).** See general procedure. All spectral data were identical to those reported for the racemic compound:<sup>16</sup> mp 220–221 °C;  $[\alpha]_{\text{D}}^{26} = +31.6$  (*c* 0.19, MeOH); Anal. ( $\text{C}_{13}\text{H}_{19}\text{N}_2\text{O}_2\text{FS}\cdot 0.25 \text{H}_2\text{O}\cdot\text{HCl}$ ) C, H, N.

**(R)-3-Fluoromethyl-7-(N-2,2,2-trifluoroethylaminosulfonyl)-1,2,3,4-tetrahydroisoquinoline Hydrochloride (R-8·HCl).** Sulfonyl chloride **14** (400 mg, 1.44 mmol) was reacted with 2,2,2-trifluoroethylamine (0.343 mL, 4.31 mmol) to afford **18** (400 mg). Lactam **18** (400 mg, 1.23 mmol) was reduced with  $\text{BH}_3\cdot\text{THF}$  (4.91 mL, 4.91 mmol) to yield (*R*)-**8**·HCl (220 mg, 44%). All spectral data were identical to those reported for the racemic compound:<sup>16</sup> mp 229–230 °C;  $[\alpha]_{\text{D}}^{26} = +40.9$  (*c* 0.25, MeOH); Anal. ( $\text{C}_{12}\text{H}_{14}\text{N}_2\text{O}_2\text{F}_3\text{S}\cdot\text{HCl}$ ) C, H, N.

**(R)-3-Fluoromethyl-7-(N-3,3,3-trifluoropropylaminosulfonyl)-1,2,3,4-tetrahydroisoquinoline Hydrochloride (R-9·HCl).** Sulfonyl chloride **14** (500 mg, 1.80 mmol) was reacted with 3,3,3-trifluoropropylamine hydrochloride (403 mg, 2.69 mmol) to afford **19** (610 mg). Lactam **19** (610 mg, 1.72 mmol) was reduced with  $\text{BH}_3\cdot\text{THF}$  (6.89 mL, 6.89 mmol) to yield (*R*)-**9**·HCl (382 mg, 57%). All spectral data were identical

to those reported for the racemic compound:<sup>16</sup> mp 236–237 °C;  $[\alpha]_{\text{D}}^{23} = +50.2$  (*c* 0.29, MeOH); Anal. ( $\text{C}_{13}\text{H}_{16}\text{N}_2\text{O}_2\text{F}_4\text{S}\cdot\text{HCl}$ ) C, H, N.

**(R)-3-Fluoromethyl-7-(N-3-methoxypropylaminosulfonyl)-1,2,3,4-tetrahydroisoquinoline Hydrochloride (R-10·HCl).** Sulfonyl chloride **14** (400 mg, 1.44 mmol) was reacted with 3-methoxypropylamine (0.440 mL, 4.32 mmol) to afford **20** (366 mg). Lactam **20** (366 mg, 1.11 mmol) was reduced with  $\text{BH}_3\cdot\text{THF}$  (4.42 mL, 4.42 mmol) to yield (*R*)-**10**·HCl (212 mg, 42%). All spectral data were identical to those reported for the racemic compound:<sup>16</sup> mp 190–191 °C;  $[\alpha]_{\text{D}}^{26} = +54.0$  (*c* 0.23, MeOH); Anal. ( $\text{C}_{14}\text{H}_{21}\text{N}_2\text{O}_3\text{FS}\cdot\text{HCl}$ ) C, H, N.

**(R)-3-Fluoromethyl-7-(N-thiomorpholinoaminosulfonyl)-1,2,3,4-tetrahydroisoquinoline Hydrochloride (R-11·HCl).** Sulfonyl chloride **14** (500 mg, 1.80 mmol) was reacted with thiomorpholine (0.543 mL, 5.40 mmol) to afford **21** (614 mg). Lactam **21** (614 mg, 1.78 mmol) was reduced with  $\text{BH}_3\cdot\text{THF}$  (7.14 mL, 7.14 mmol) to yield (*R*)-**11**·HCl (328 mg, 62%). All spectral data were identical to those reported for the racemic compound:<sup>16</sup> mp 224–225 °C;  $[\alpha]_{\text{D}}^{26} = +49.7$  (*c* 0.24, MeOH); Anal. ( $\text{C}_{14}\text{H}_{19}\text{N}_2\text{O}_3\text{FS}_2\cdot\text{HCl}$ ) C, H, N.

**Acknowledgment.** This research was supported by NIH Grant HL 34193. The 500 MHz NMR spectrometer was partially funded by the National Science Foundation through grant CHE-9977422. We thank Sarah Neuenswander of the University of Kansas NMR laboratory (NSF Grant CHE-9977422) for obtaining <sup>19</sup>F spectra and Dr. Gerald Lushington of the University of Kansas molecular graphics and modeling laboratory for helpful discussions concerning the conformational analysis.

**Supporting Information Available:** Results for elemental analyses (C, H, N) for assayed compounds are included. This material is available free of charge via the Internet at <http://pubs.acs.org>.

## References

- (1) This work was presented at the 226th National Meeting of the American Chemical Society, New York, Sept 7–11, 2003 (MEDI-135). The contents of this paper were taken in large part from the Ph.D. dissertation (University of Kansas, 2004) of F.A.R.
- (2) Axelrod, J. Purification and Properties of Phenylethanolamine N-Methyltransferase. *J. Biol. Chem.* **1962**, *237*, 324–333.
- (3) Vogt, M. The Concentration of Sympathin in Different Parts of the Central Nervous System Under Normal Conditions and After the Administration of Drugs. *J. Physiol.* **1954**, *123*, 451–481.
- (4) Burke, W. J.; Chung, H. D.; Strong, R.; Mattammal, M. B.; Marshall, G. L.; Nakra, R.; Grossberg, G. T.; Haring, J. H.; Joh, T. H. Mechanism of Degeneration of Epinephrine Neurons in Alzheimer's Disease. In *Central Nervous System Disorders of Aging: Clinical Intervention and Research*; Strong, R., Ed.; Raven Press: New York, 1988; pp 41–70.
- (5) Kennedy, B. P.; Bottiglieri, T.; Arming, E.; Ziegler, M. G.; Hansen, L. A.; Masliah, E. Elevated S-Adenosylhomocysteine in Alzheimer Brain: Influence on Methyltransferases and Cognitive Function. *J. Neural Transm.* **2004**, *111*, 547–567.
- (6) Saavedra, J. M.; Grobecker, H.; Axelrod, J. Adrenaline-Forming Enzyme in Brainstem: Elevation in Genetic and Experimental Hypertension. *Science* **1976**, *191*, 483–484.
- (7) Rothballer, A. B. The Effects of Catecholamines on the Central Nervous System. *Pharmacol. Rev.* **1959**, *11*, 494–547.
- (8) Goldstein, M.; Lew, J. Y.; Matsumoto, Y.; Hokfelt, T.; Fuxe, K. Localization and Function of PNMT in the Central Nervous System. In *Psychopharmacology: A Generation of Progress*; Lipton, M. A., DiMascio, A., Killam, K. F., Eds.; Raven Press: New York, 1978; pp 261–269.
- (9) Stone, E. A.; Grunewald, G. L.; Lin, Y.; Ashan, R.; Rosengarten, H.; Kramer, H. K.; Quartermain, D. Role of Epinephrine Stimulation of CNS  $\alpha_1$ -Adrenoceptors in Motor Activity in Mice. *Synapse* **2003**, *49*, 67–76.
- (10) Rosin, D. L.; Zeng, D.; Stornetta, R. L.; Norton, F. R.; Riley, T.; Okusa, M. D.; Guyenet, P. G.; Lynch, K. R. Immunohistochemical Localization of  $\alpha_2$ -Adrenergic Receptors in Catecholaminergic and Other Brainstem Neurons in the Rat. *Neuroscience* **1993**, *56*, 139–155.
- (11) Stolk, J. M.; Vantini, G.; Guchait, R. B.; U'Prichard, D. C. Strain Differences in Rat Brain Epinephrine Synthesis: Regulation of  $\alpha_2$ -Adrenergic Receptor Number by Epinephrine. *Science* **1983**, *221*, 1297–1299.

- (12) Grunewald, G. L.; Caldwell, T. M.; Li, Q.; Slavica, M.; Criscione, K. R.; Borchardt, R. T.; Wang, W. Synthesis and Biochemical Evaluation of 3-Fluoromethyl-1,2,3,4-tetrahydroisoquinolines as Selective Inhibitors of Phenylethanolamine *N*-Methyltransferase versus the  $\alpha_2$ -Adrenoceptor. *J. Med. Chem.* **1999**, *42*, 3588–3601.
- (13) Audus, K. L.; Borchardt, R. T. Characterization of an In Vitro Blood-Brain Barrier Model System for Studying Drug Transport and Metabolism. *Pharm. Res.* **1986**, *3*, 81–87.
- (14) Takakura, Y.; Audus, K. L.; Borchardt, R. T. Blood-Brain Barrier: Transport Studies in Isolated Brain Capillaries and in Cultured Brain Endothelial Cells. *Adv. Pharmacol.* **1991**, *22*, 137–165.
- (15) ClogP values were calculated with the ClogP function in SYBYL.
- (16) Romero, F. A.; Vodonick, S. M.; Criscione, K. R.; McLeish, M. J.; Grunewald, G. L. Inhibitors of Phenylethanolamine *N*-Methyltransferase That Are Predicted To Penetrate the Blood-Brain Barrier: Design, Synthesis and Evaluation of 3-Fluoromethyl-7-(*N*-substituted aminosulfonyl)-1,2,3,4-tetrahydroisoquinolines That Possess Low Affinity toward the  $\alpha_2$ -Adrenoceptor. *J. Med. Chem.* **2004**, *47*, 4483–4493.
- (17) Martin, J. L.; Begun, J.; McLeish, M. J.; Caine, J. M.; Grunewald, G. L. Getting the Adrenaline Going: Crystal Structure of the Adrenaline-Synthesizing Enzyme PNMT. *Structure* **2001**, *9*, 977–985.
- (18) Grunewald, G. L.; Caldwell, T. M.; Li, Q.; Dahanukar, V. H.; McNeil, B.; Criscione, K. R. Enantiospecific Synthesis of 3-Fluoromethyl-, 3-Hydroxymethyl-, and 3-Chloromethyl-1,2,3,4-tetrahydroisoquinolines as Selective Inhibitors of Phenylethanolamine *N*-Methyltransferase versus the  $\alpha_2$ -Adrenoceptor. *J. Med. Chem.* **1999**, *42*, 4351–4361.
- (19) Compounds **4**, **5**, (*R*)-**4** and (*R*)-**5** were converted to their methoxy- $\alpha$ -trifluoromethylphenylacetamide derivatives by Mosher's method. Compounds (*R*)-**4** and (*R*)-**5** were > 95% ee as determined by examination of the fluoromethyl peak in the  $^{19}\text{F}$  NMR spectra. Restricted rotation of the acetamide precluded analysis of the trifluoromethyl peak.
- (20) Caine, J. M.; Macreadie, I. G.; Grunewald, G. L.; McLeish, M. J. Recombinant Human Phenylethanolamine *N*-Methyltransferase: Overproduction in *Escheria coli*, Purification and Characterization. *Protein Expression Purif.* **1996**, *8*, 160–166.
- (21) Grunewald, G. L.; Borchardt, R. T.; Rafferty, M. F.; Krass, P. Conformationally Defined Adrenergic Agents. 5. Conformational Preferences of Amphetamine Analogues for Inhibition of Phenylethanolamine *N*-Methyltransferase. *Mol. Pharmacol.* **1981**, *20*, 377–381.
- (22) U'Prichard, D. C.; Greenberg, D. A.; Snyder, S. H. Binding Characteristics of a Radiolabeled Agonist and Antagonist at Central Nervous System Alpha Noradrenergic Receptors. *Mol. Pharmacol.* **1977**, *13*, 454–473.
- (23) Ibanez, A. F.; Iglesias, G. Y. M.; Delfino, J. M. Conformational Analysis of 1,2,3,4-Tetrahydroisoquinolines. *J. Heterocycl. Chem.* **1996**, *33*, 265–270.
- (24) Lankin, D. C.; Grunewald, G. L.; Romero, F. A.; Oren, I. Y.; Snyder, J. P. The NH–FC Dipole Orientation Effect for Pendant Exocyclic  $\text{CH}_2\text{F}$ . *Org. Lett.* **2002**, *4*, 3557–3560.
- (25) Grunewald, G. L.; Caldwell, T. M.; Li, Q.; Criscione, K. R. Synthesis and Evaluation of 3-Trifluoromethyl-7-substituted-1,2,3,4-tetrahydroisoquinolines as Selective Inhibitors of Phenylethanolamine *N*-Methyltransferase versus the  $\alpha_2$ -Adrenoceptor. *J. Med. Chem.* **1999**, *42*, 3315–3323.
- (26) Fuller, R. W.; Molloy, B. B.; Day, W. A.; Roush, B. W.; Marsh, M. M. Inhibition of Phenylethanolamine *N*-Methyltransferase by Benzylamines. 1. Structure–Activity Relationships. *J. Med. Chem.* **1973**, *16*, 101–106.
- (27) Frisch, M. J.; Trucks, G. W.; Schlegel, H. B.; Scuseria, G. E.; Robb, M. A.; Cheeseman, J. R.; Zakrzewski, V. G.; Montgomery, J. A., Jr.; Stratmann, R. E.; Burant, J. C.; Dapprich, S.; Millam, J. M.; Daniels, A. D.; Kudin, K. N.; Strain, M. C.; Farkas, O.; Tomasi, J.; Barone, V.; Cossi, M.; Cammi, R.; Mennucci, B.; Pomelli, C.; Adamo, C.; Clifford, S.; Ochterski, J.; Petersson, G. A.; Ayala, P. Y.; Cui, Q.; Morokuma, K.; Malick, D. K.; Rabuck, A. D.; Raghavachari, K.; Foresman, J. B.; Cioslowski, J.; Ortiz, J. V.; Stefanov, B. B.; Liu, G.; Liashenko, A.; Piskorz, P.; Komaromi, I.; Gomperts, R.; Martin, R. L.; Fox, D. J.; Keith, T.; Al-Laham, M. A.; Peng, C. Y.; Nanayakkara, A.; Gonzalez, C.; Challacombe, M.; Gill, P. M. W.; Johnson, B. G.; Chen, W.; Wong, M. W.; Andres, J. L.; Head-Gordon, M.; Replogle, E. S.; Pople, J. A. *Gaussian 98, revision A.9*; Gaussian, Inc.: Pittsburgh, PA, 1998.
- (28) The initial ligand structure for docking was the geometry optimized structure as shown in Figure 3. However, AutoDock optimizes the fluorine-Tyr222 interaction and thus in several cases a different rotamer appears in Figures 4 and 5. The energy that is lost upon C–C(F) rotation (ca. 0.01 kcal/mol) is minimal compared to the energy gained by interaction with the enzyme.
- (29) Grunewald, G. L.; Sall, D. J.; Monn, J. A. Conformational and Steric Aspects of the Inhibition of Phenylethanolamine *N*-Methyltransferase by Benzylamines. *J. Med. Chem.* **1988**, *31*, 433–444.
- (30) (a) SigmaPlot for Windows 2001, version 7.0, SPSS, Inc., Chicago, IL. (b) Enzyme Kinetics Module, version 1.1, SPSS, Inc., Chicago, IL.
- (31) Morris, G. M.; Goodsell, D. S.; Halliday, R. S.; Hart, W. E.; Belew, R. K.; Olson, A. J. Automated Docking Using a Lamarckian Genetic Algorithm and an Empirical Binding Free Energy Function. *J. Comput. Chem.* **1998**, *19*, 1639–1662.

JM049594X